

Experimental Report MI-1285

Characterization of mono- and poly-crystalline diamond detectors for hadron therapy and high energy physics applications

Summary

In the framework of two collaborations aiming at the development of high-energy particle detectors and hadron therapy monitoring, mono- and poly-crystalline diamond detectors and their front-end electronics have been characterized. In the ESRF 4-bunch short-pulsed mode, the X-ray pulses mimic the passage of single ionizing particles. We characterized the temporal and charge/current signal responses of several diamond detector prototypes over a large fraction of their surfaces with:

- sub-nanosecond timing using large bandwidth acquisition of pulse waveforms (digital sampling oscilloscopes) synchronized with the storage ring time structure,
- micron spatial resolutions, using a current integration acquisition mode.

Diamonds with aluminium disk-shaped surface metallization and double-side stripped metallized diamonds were both tested using the XBIC (X Rays Beam Induced Current) set-up of the ID21 beamline. This enables us to evaluate the capability of diamond to be used as position sensitive detector with a fast timing response at the order of few tens of picoseconds. These experiments were successful. MI-1285 led to the conclusions that narrower inter-strip bands should be used and that electronics should be tuned with lower noise level, in order to improve our timing resolution well below 100 ps. Further characterizations are necessary for the use of such detectors using time-resolved XBIC at ESRF.

Experimental set-up

XBIC is of huge interest for our application. In our experiment, a 8.5 keV photon focused micro-beam with a well-defined time structure was used. As regards energy deposition in the diamond, 35 % of the beam is absorbed in 300 μm diamond material, which makes the energy deposit almost constant and continuous along the beam path. In the ESRF 4-bunch mode, the ~ 100 ps duration X-ray pulses, containing a fixed number of photons, adjustable by means of attenuators (maximum value of ~ 1400), mimic the passage of single ionizing particles (maximum energy deposit ~ 4.1 MeV). Photon bunches are separated by 704 ns intervals, which makes possible individual pulse response measurement, as well as continuous current integration with picoammeters.

The sensor contact for the disk-shaped metallization consists of a 50 nm thick aluminum layer deposited on both sides. Diamonds are mounted on sample holders with 50 Ω adapted impedance and SMA connectors, enabling reversible bias and signal readout from both sides of the diamond as illustrated by

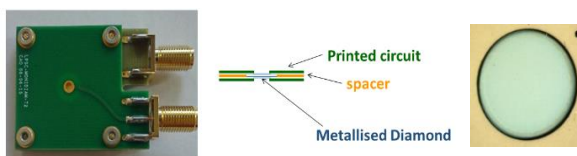


Fig. 1 The diamond sensor with a disk-shaped metallization housed in its socket.

Fig. 1. The signals are amplified with a CIVIDEC C2 low-noise broadband RF amplifier (2 GHz, 40 dB). It exhibits a $50\ \Omega$ input impedance and is able to work with less than 1 ns FWHM pulse widths.

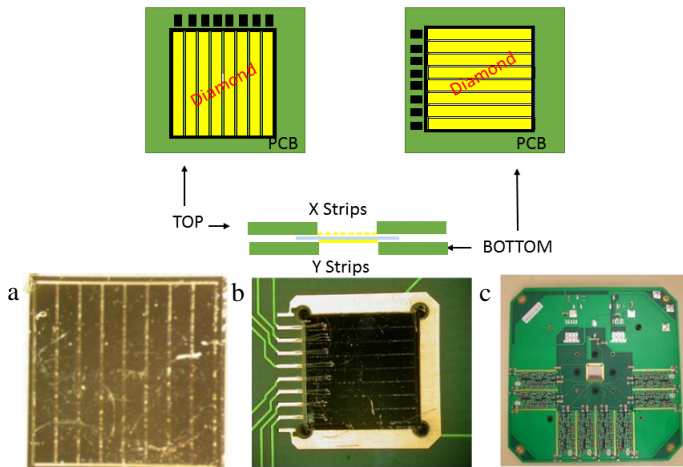


Fig. 2 Top: scheme of the double-side stripped diamond sensor housed in its dual PCB holder and its read-out electronics. Bottom: details of the diamond stripped metallization and the wire bonding connection of the diamond to the PCB. (For more information, see text).

A double-side strip metallization of the diamond sensors was performed for a position sensitive detector development (one side in X direction and the other in Y direction, see Fig. 2). The lift-off process was used to create the strips. It consists in creating structures (patterning) using a sacrificial material (e.g., photoresist). This was performed at the NANOFAB laboratory from the Néel Institute. Four steps are needed to perform the strip metallization. At first, S1818 photoresist is deposited on the substrate ($10 \times 10\ \text{mm}^2$ diamond). Then the pattern is exposed thanks to an extreme ultraviolet lithography (laser wavelength 405 nm). Development will dissolve exposed pattern. The sample is then metallized with a 100 nm aluminium layer. Residual photoresist is finally lifted away in a solvent with the parts of the undesired metallization. The resulting metallization on the diamond sensor consists of 8 strips of 1 mm width separated by a $100\ \mu\text{m}$ gap and surrounded by a guard ring (Fig. 2 a). Unlike the case of the disk-shaped metallization, wire bonding ensures the electrical connection between each diamond strip and the PCB (Fig. 2 b). In addition, a set of discrete current amplifiers designed at LPSC (1 GHz, 30 dB) are mounted on the circuit board (Fig. 2 c). The whole set-up is placed inside an electromagnetic shielding box surrounded by SMA connectors to enable bias and signal readout (Fig. 3).

The diamond samples were placed inside an electromagnetic shielding box (Fig. 3). The box was positioned with micrometric reproducibility at the sample position of the micro-diffraction end-station (in air) of the ID21 beamline at ESRF. The pulse shape readout mode was performed with a 500 MHz, 3.2 GS/s digital sampling 'Wavecatcher' system from LAL/IRFU. This system could be configured in a continuous acquisition mode, recording a set of waveforms, and thus enabling large statistics offline analysis. In addition, a 2 GHz, 20 GS/s analog bandwidth DSO (Digital Sampling Oscilloscope LeCroy

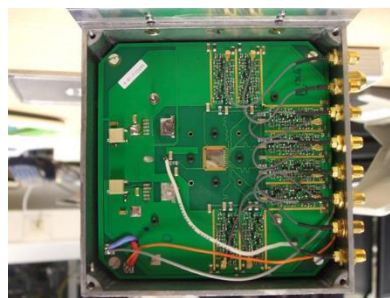
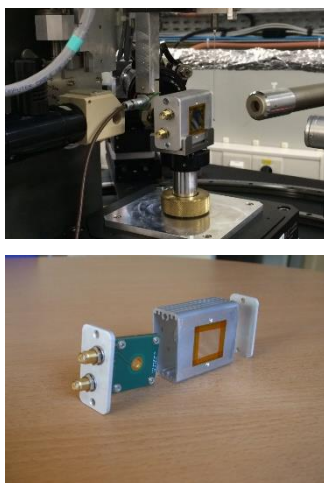
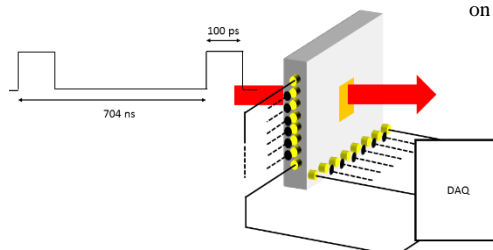


Fig. 3 ESRF experimental test bench. Left top: diamond detector mounting inside EM-shielding box positioned on the ESRF ID21 beam line, Left bottom: the diamond sensor with a disk-shaped metallization housed in its socket. Right top: the $1\ \text{cm}^2$ double side stripped diamond mounted on the PCB inside an electromagnetic shielding box. 8 discrete preamplifiers are mounted on each side. Right bottom: scheme of the box positioned on the ESRF ID21 beam line.



620Zi) was used. The DSO data acquisition was fully integrated into the ESRF ID21 SPEC software acquisition framework which enabled us to measure the temporal response of the detectors as they were scanned in the beam, thus creating 2D response maps over the detector surfaces.

Results

1.) Time resolution measurement with disk-shaped metallized diamonds

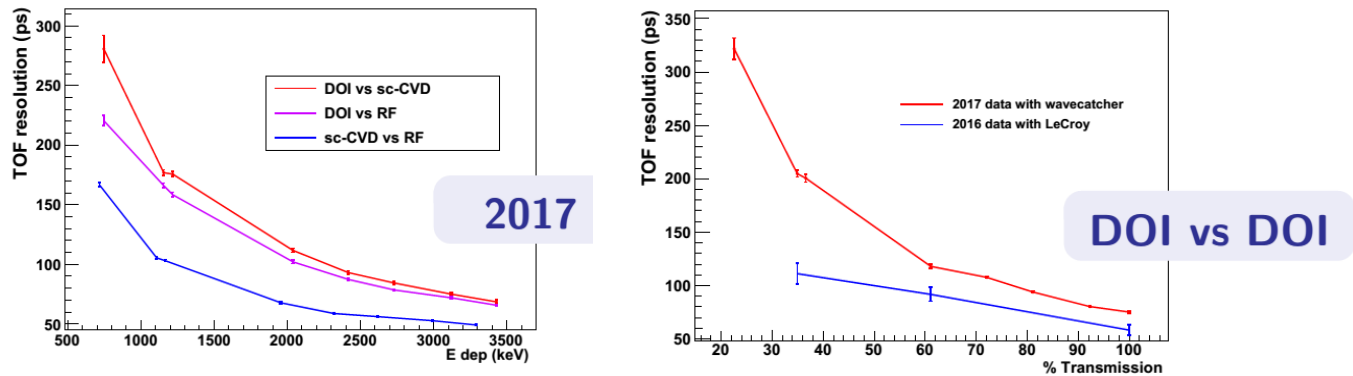


Fig. 4 Time resolution. Left : measured on a $5.0 \times 5.0 \text{ mm}^2 \times 300 \mu\text{m}$ Diamond On Iridium detector (DOI) and a $4.5 \times 4.5 \text{ mm}^2 \times 518 \mu\text{m}$ sc-CVD (Single Crystal Chemical Vapor Deposition) diamond (E6) as a function of the energy deposited in the detector per photon bunch Right : measured between both faces of a $5.0 \times 5.0 \text{ mm}^2 \times 300 \mu\text{m}$ DOI detector : comparison between 2016 and 2017 data.

Time-of-Flight measurements were done between a $5.0 \times 5.0 \text{ mm}^2 \times 300 \mu\text{m}$ Diamond On Iridium (DOI) and a $4.5 \times 4.5 \text{ mm}^2 \times 518 \mu\text{m}$ sc-CVD (Single Crystal Chemical Vapor Deposition) diamond (E6), see Fig. 4. They were both set in a metallic box. Data acquisition was done with the Wavecatcher system. The beam Radio-Frequency (RF) signal was used as a trigger. Different attenuators made of aluminum and titanium plates with different thicknesses were used to modify the incident photon flux. By varying the incident flux, one can vary the energy deposited in the diamond detectors. For each curve, the minimal time resolution is obtained with no attenuation of the photon beam. One can observe that the achievable time resolution depends on the energy deposited in the detector. Indeed, it depends on the signal-to-noise ratio.

On the right part of Fig. 4 a comparison is made for the time resolution measured with an identical test bench set-up (same diamond and same CIVIDEC preamplifiers connected to both detector faces) in 2016 and in 2017 both on ID21. It is obvious that due to a higher noise level, the 2017 results are not optimal. This must be further investigated.

2.) Characterization of double-side stripped diamond detectors

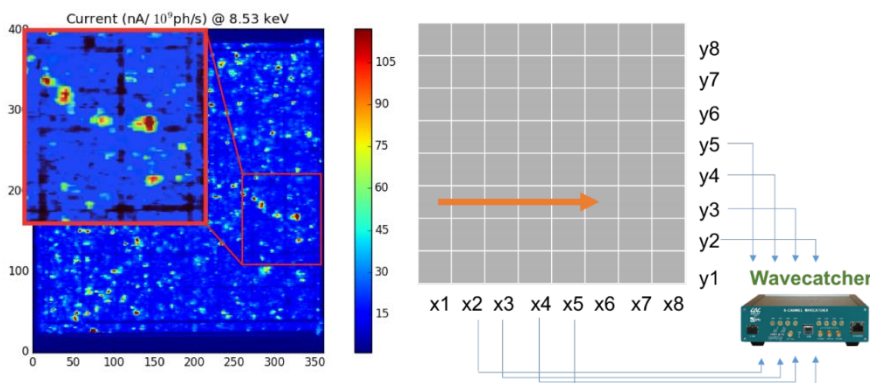


Fig. 5 : Left: current-response map of a 1cm^2 polycrystalline diamond detector, double-side stripped (8 strips/side). The inset enables the observation of the charge collection defect along strip interfaces. Right: detector scanning with XBIC $100 \mu\text{m}$ steps off line analysis of digitized signals

We have performed an X-Ray analysis of a double-side stripped diamond surface in a current integration mode (Fig. 5). The non-uniformity of the diamond response, quantified by the color scale, reflects the defects distribution in the material. A zoom on an about $2 \times 2 \text{ mm}^2$ area is superimposed. An ad-hoc adjustment of the colour scale makes visible the inter-strip regions, corresponding to a decrease of the charge collection efficiency. This already shows that narrower gaps should be used in order to keep the efficiency constant.

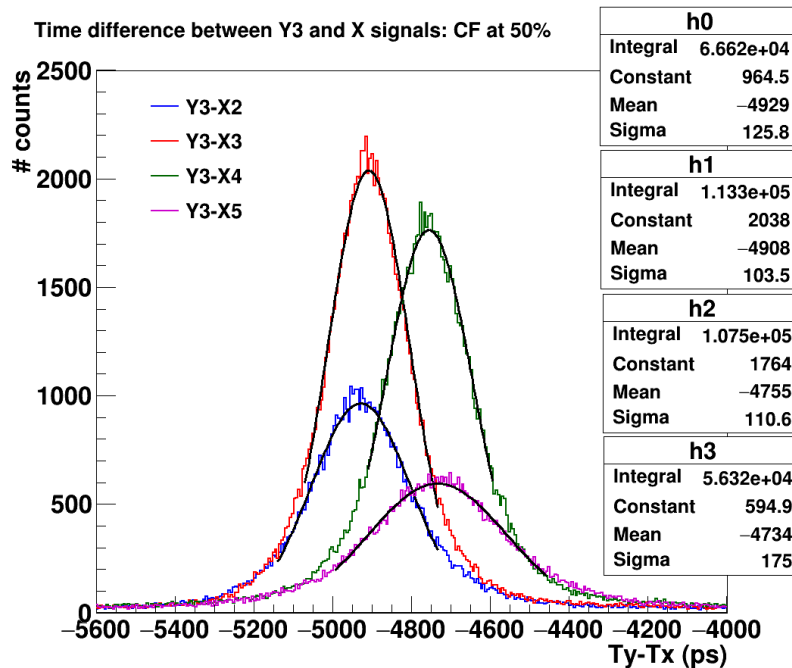


Fig. 6 Distributions of the time difference between Y strip and X strips obtained with an offline Constant Fraction (CF) discrimination method at a 50 % level.

On Fig. 6 a time resolution measurement was done between Y and X strips while the stripped diamond detector was motor scanned in the beam with $100 \mu\text{m}$ steps as explained on the scheme of Fig. 5. Note that the typical values of $\sim 200\text{ns}$ rms time resolution were intentionally degraded in order to adapt the preamplifier bandwidth during the experiment. They correspond to the quadratic sum of both channels resolutions. Such results are encouraging and demonstrated the feasibility of a position sensitive and high time resolution beam tagging hodoscope based on diamonds.

These are preliminary results; a more refined analysis will be performed in a near future, in particular to quantify the cross talk and the reconstructed spatial resolution.

Scientific production and perspectives :

The results were presented at the following international conferences : IEEE-NSS-MIC in November 2016¹, ANIMMA in June 2017 (invited talk - proceedings to be published in IEEE) as well as HEP 2017 in July 2017 and ICNTRM in August 2017. We foresee a publication in the corresponding IEEE-TNS journal by the end of 2017-begining of 2018.

We are now considering further developments of large area detectors provided by Augsburg Univ. with appropriate strip metalization. The respective influence of interstrip capacitance and neighbouring electronic readout channels on the cross talk is still under analysis, this will lead to an optimal strip size. Also, we have to better define the time-resolution versus the diamond detector transmission. Further measurements are necessary, including ASIC electronics readout, and are the subject of the new proposal on ID16b.

¹ “Large Area Polycrystalline Diamond Detectors for Online Hadron Therapy Beam Tagging Applications” ML. Gallin-Martel et al, proceedings IEEE-NSS-MIC 2016, <https://hal.archives-ouvertes.fr/PRIMES/hal-01436786v1>